Published in final edited form as:
Phytochem Lett. 2011 December 1; 4(4): 426–431. doi:10.1016/j.phytol.2011.07.009.

Suppression of cyclooxygenase-2 and inducible nitric oxide synthase expression by epimuqubilin A via IKK/IκB/NF-κB pathways in lipopolysaccharide-stimulated RAW 264.7 cells

Eun-Jung Park, **Sarot Cheenpracha**, **Leng Chee Chang**, and **John M. Pezzuto***
College of Pharmacy, University of Hawaii at Hilo, 34 Rainbow Drive, Hilo, HI, 96720, USA

Abstract

Lipopolysaccharide (LPS)-stimulated RAW 264.7 cells are commonly used as a model for assessing the anti-inflammatory or chemopreventive potential of test compounds. Epimuqubilin A, a norsesterterpene peroxide isolated from marine sponge *Latrunculia* sp., inhibits nitric oxide production in LPS-stimulated RAW 264.7 cells (IC_{50} = 7.6 μM). At both the mRNA and protein levels, cyclooxygenase-2 (COX-2) and inducible nitric oxide synthase (iNOS) are suppressed in a dose-dependent manner. Mitogen-activated protein kinases (MAPKs), one major upstream signaling pathway involved in the transcription of both COX-2 and iNOS, were not affected by treatment of epimuqubilin A. However, the compound blocked the phosphorylation of inhibitor κB (IκB) kinase (IKKβ), resulting in the stabilization of IκBα, and inhibition of NF-κB p65 nuclear translocation and DNA binding. Levels of phosphorylated IKKα were not affected. This is an unique mechanistic relationship that suggests epimuqubilin A warrants further exploration as a potential therapeutic agent.

Keywords

Norsesterterpene peroxide; Epimuqubilin A; Cyclooxygenase-2; Inducible nitric oxide synthase; Inhibitor κB kinase; RAW 264.7

1. Introduction

Marine sponges have been received attention as sources of novel leads for the development of therapeutic agents due to species and chemical diversity (Thomas et al., 2010). A broad range of extracts and compounds from marine sponges have been reported with bioactivities. For example, more than 2000 publications are revealed by a search of PubMed using the key term ‘marine sponge’ (February 2011). In terms of clinical application, cytarabine (Ara-C) and vidarabine (Ara-A), originally derived from marine sponge *Cryptotethia crypta*, received FDA approval as anticancer and antiviral agents (Yasuhara-Bell and Lu, 2010). More recently, some compounds have been entered into clinical trials as anticancer drug candidates, including eribulin mesylate (E7389) in a phase III trial, and E7974 (hemiasterlin) in phase I trial (Mayer et al., 2010). Some extracts or compounds from marine sponges have been reported to inhibit the inflammation processes, including an ethyl acetate fraction from *Cliona celata* (Yang et al., 2010), the extract from *Aplysina caissara* (Azevedo et al., 2008), halichlorine (Tsubosaka et al., 2010), and heteronemin (Schumacher et al., 2010). We have demonstrated the anti-inflammatory potential of epimuqubilin A, a

*Corresponding author. Tel.: +1 808 933 2909; fax: +1 808 933 2981. pezzuto@hawaii.edu (J.M. Pezzuto).

norsesterterpene peroxide isolated from marine sponge *Latrunculia* sp. (C006879), by means of inhibiting nitric oxide (NO) production (Cheenpracha et al., 2010).

Nitric oxide (NO), endogenously synthesized by the oxidation of L-arginine, is known to participate in various physiological processes including vasodilation, neurotransmission, anti-platelet aggregation, and anti-oxidation of low density lipoprotein cholesterol (Fukumura et al., 2006; Förstermann, 2010). However, the aberrant production of NO can lead to various diseases states, including cancer, heart failure, atherosclerosis, ischemic stroke, diabetes, chronic obstructive pulmonary disease, asthma, arthritis, neurodegenerative diseases, multiple sclerosis, cirrhosis, ulcerative colitis, and Crohn's disease (Fukumura et al., 2006; Kanwar et al., 2009). The generation of NO is catalyzed by nitric oxide synthase (NOS), of which there are three isoforms: neuronal NOS (nNOS, NOS1), inducible NOS (iNOS, NOS2), and endothelial NOS (eNOS, NOS3). Inducible NOS is of particular concern since it is frequently responsible for NO production associated with patho-physiological conditions. Notably, a considerable number of studies have demonstrated the key role of NO and iNOS in tumor pathology through various stages including tumor initiation, promotion, and progression (e.g., angiogenesis, tumor cell growth, and invasion) (Kanwar et al., 2009). The expression of iNOS is increased in many solid tumors (Ambs et al., 1998; Aggarwal and Gehlot, 2009), including gastric (Rajnakova et al., 2001), brain (Broholm et al., 2003), esophagus (Wilson et al., 1998), melanoma (Ekmekcioglu et al., 2006) and urothelial carcinomas (Hayashi et al., 2001). Several mechanisms of involvement of NO and metabolites in tumor biology have been proposed, including DNA damage and subsequent gene mutation (e.g., tumor suppressor p53), suppression of DNA repair enzymes (e.g., human thymine-DNA glycosylase and 8-oxoguanine DNA glycosylase), and *S*-nitrosylation of caspases (Fukumura et al., 2006).

Another important mediator involved in the process of inflammation and carcinogenesis is cyclooxygenase (COX)-2. Cyclooxygenases are known to catalyze the rate-limiting step in the biosynthesis of prostaglandins which have been reported to function in various physiological processes including modulation of immune responses, protection of gastrointestinal mucosa, maintenance of renal homeostasis and regulation of blood coagulation (Greenhough et al., 2009). However, a growing body of evidence suggests COX-2 is involved in carcinogenesis. Indeed, the over-expression of COX-2 has been reported in leukemia, gastrointestinal cancers, genitourinary cancers, breast cancer, gynecologic cancers, and head and neck cancers (Aggarwal and Gehlot, 2009).

In this study, we have investigated the underlying mechanism by which epimuqubilin A inhibits NO production, in association with COX-2 and iNOS, and upstream signaling molecules including MAPKs and NF-κB.

2. Results

2.1. Inhibitory effect of epimuqubilin A on LPS-induced nitrite production in RAW 264.7 cells

As shown in Fig. 1B, untreated macrophages released a basal level of nitrite (0.05 ± 0.00 μM) into the media of cultured RAW 264.7 cells, whereas LPS treatment (20 h) greatly increased nitrite production (33.67 ± 2.09 μM). Epimuqubilin A inhibited LPS-induced nitrite production in a dose-dependent manner, yielding an IC_{50} value of 7.61 μM. As judged by the SRB assay, epimuqubilin A did not mediate a cytotoxic response under any of these experimental conditions. The results are consistent with our original report (IC_{50} = 7.4 μM) (Cheenpracha et al., 2010).

2.2. Inhibitory effects of epimuqubilin A on LPS-induced protein and mRNA expression of COX-2 and iNOS

The effect of epimuqubilin A on the expression of iNOS and COX-2 was examined in LPS-stimulated RAW 264.7 cells. RAW 264.7 cells were pretreated with various concentrations of epimuqubilin A for 15 min and further incubated with LPS (1 μg/mL) for 18 h prior to the evaluation of protein expression or 5 h prior to the evaluation of mRNA expression. As illustrated in Fig. 2A, epimuqubilin A suppressed the expression of COX-2 and iNOS dose-dependently at both the protein and mRNA levels, with significant differences (Fig. 2B). The expression of β-actin, one of the 'housekeeping' genes used as a loading control, was not changed.

2.3. Effect of epimuqubilin A on the MAPK pathway

To further examine the molecular mechanism underlying epimuqubilin A-mediated inhibition of COX-2 and iNOS, cellular levels of upstream signaling molecules, phosphorylated and total MAPKs, were determined. RAW 264.7 cells were pretreated with epimuqubilin A for 15 min, and stimulated with LPS (1 μg/mL) for 15 min. As shown in Fig. 3, LPS treatment induced the phosphorylation of MAPKs, including p-p38 MAPK, p-ERK1/2, and p-SAPK/JNK. However, epimuqubilin A did not significantly affect the total or phosphorylated of MAPKs.

2.4. Effect of epimuqubilin A on the NF-κB pathway

Next, we examined the effect of epimuqubilin A on the NF-κB pathway. First, the protein levels of NF-κB p65, the major subunit of NF-κB, were examined in nuclear fractions. The NF-κB p65 subunit was increased in nuclear fractions after 1 h of treatment with LPS (1 μg/mL) (Fig. 4A). Consistent with this, stimulation of the cells with LPS (1 μg/mL) for 1.5 h resulted in increased binding of NF-κB and the corresponding DNA, as demonstrated by increased band intensity (Fig. 4B). In a concentration-dependent manner, treatment with epimuqubilin A attenuated the nuclear increase of NF-κB p65 protein levels, as well as the interaction of NF-κB and DNA. No effect on lamin A/C, the nuclear loading control, was observed, and the addition of an excessive amount of specific unlabeled consensus oligonucleotide (competitor) completely inhibited the band shifts with IRDye® 700 infrared dye-5′-end-labelled NF-κB, showing the specificity of the protein–DNA interaction.

Nuclear translocation of NF-κB occurs after release from IκBs. Therefore, the level of IκBα was examined by Western blot analyses. As shown in Fig. 4C, treatment with LPS led to IκBα degradation, and this was completely blocked by epimuqubilin A in a concentration-dependent manner. This response correlated with the inhibition of IKKβ phosphorylation, whereas no effects were observed on LPS-induced phosphorylation of IKKα.

3. Discussion

Norsesterterpene peroxides like epimuqubilin A, unique marine metabolites mainly found in marine sponges, have shown anti-inflammatory (Cheenpracha et al., 2010), anti-malarial, anti-viral, anti-toxoplasma (El Sayed et al., 2001) activities, as well as cytotoxic activities toward various cancer cells (Sperry et al., 1998; Youssef et al., 2001; Phuwapraisirisan et al., 2003; Youssef, 2004; Dai et al., 2007; Ibrahim et al., 2008). Nonetheless, there are relatively few studies reported on norsesterterpene peroxides, probably due to difficulties in obtaining sufficient amounts of materials. Therefore, we thought it would be of value to assess the underlying mechanisms of epimuqubilin A which was previously reported to inhibit NO production in LPS-stimulated murine macrophages (Cheenpracha et al., 2010).

Since the large amount of NO production in LPS-stimulated cells (33.67 ± 2.09 μM) compared with that in resting cells (0.05 ± 0.00 0μM) is mainly due to increased expression of iNOS (which facilitates the production of NO from L-arginine and oxygen), we determined whether the inhibitory activity of epimuqubilin A on NO production results from a reduction in the expression of iNOS protein and mRNA levels. Inducible NOS is known to be primarily controlled by transcriptional and translational mechanisms, rather than post-translational mechanisms (e.g., modification and degradation) (Pautz et al., 2010). In addition, we examined COX-2, another major enzyme which is induced by LPS stimulation, and known to be related to inflammatory processes as well as carcinogenesis. Epimuqubilin A exerted inhibitory activity on the expression of both COX-2 and iNOS. We further examined the upstream molecules involved in transcriptional regulation of COX-2 and iNOS: MAPKs and IKK/IκBα/NF-κB. MAPKs, including p38 MAPK, ERK1/2, and SAPK/JNK, are activated after phosphorylation of specific sites (Thr180/Tyr182 for p38 MAPK, Thr202/Tyr204 for ERK1/2, Thr183/Tyr185 for SAPK/JNK). In non-stimulated RAW 264.7 cells, the phosphorylated levels of MAPKs are nearly undetectable by Western blot analysis (Fig. 3). LPS induces the phosphorylation of MAPKs, but epimuqubilin A did not attenuate the response, indicating a lack of mechanistic relevance.

Next, we examined the possible effect of epimuqubilin A on the activation of NF-κB, which is known to function as a transcriptional factor in expression of COX-2 and iNOS (Hussain and Harris, 2007). NF-κB mediates various physiological processes, but dysregulated NF-κB activation is involved in a wide range of diseases and disorders in cardiovascular, gastrointestinal, hepatic, neurologic, pulmonary, and renal systems. In particular, it has been reported that NF-κB plays pivotal roles in inflammatory diseases and cancers (Liu and Malik, 2006). NF-κB exists as homo- or heterodimers with a combination of five subunits including RelA (p65), NF-κB1 (p50; p105), NF-κB2 (p52; p100), c-Rel, and RelB. The major form of NF-κB is a heterodimer consisting of the p65 subunit with either p50 or p52 subunits; p65 and p50 are expressed ubiquitously in various cell types (Li and Verma, 2002). Therefore, as the first step to explore effects on NF-κB signaling, we examined the level of p65 as a major subunit of NF-κB in nucleus, since nuclear localization of NF-κB is an important marker of activation. After LPS stimulation, the levels of p65 in nuclear fractions increased in comparison with control cells. Epimuqubilin A inhibited nuclear translocation of p65 in a concentration-dependent manner. Subsequently, the binding activity of NF-κB on NF-κB binding site (*cis*-acting element) in the promoter region was inhibited.

Further, IκB is known to play a key role in nuclear translocation of NF-κB. In the quiescent state, IκB family members are bound to NF-κB, and sequestered in the cytoplasm. Different members of the IκB family have been reported, such as IκBα, IκBβ, IκBγ, IκBε, IκBαζ, Bcl-3, p105 (NF-κB1), p100 (NF-κB2), and molecule possessing ankyrin-repeats induced by lipopolysaccharide (MAIL). Among them, IκBα, IκBβ, and IκBε have the NH_2-terminal regulatory domain necessary for IκB degradation (Liu and Malik, 2006), with IκBα being reported as crucial in regard to NF-κB activation and translocation into the nucleus (Ferreiro and Komives, 2010). Once cells are treated with LPS, both IκBα and IκBβ undergo ubiquitin-dependent protein degradation, resulting in the release and nuclear translocation of NF-κB (Li and Verma, 2002; Liu and Malik, 2006). Therefore, protein levels of IκBα were examined, and it was found that epimuqubilin A inhibited the degradation of IκBα after LPS treatment.

IκBα degradation results from the phosphorylation of specific serine sites and IKK catalyzes this step. The IKK complex is composed of catalytic (IKKα and IKKβ) and regulatory subunits (IKKγ) (Oeckinghaus and Ghosh, 2009). We investigated the effect of

epimuqubilin A on the activation of IKK in LPS-stimulated RAW 264.7 cells, and observed a reduction in p-IKKβ levels.

These findings suggest that epimuqubilin A reduces iNOS and COX-2 expression through inhibiting the NF-κB pathway, specifically by blocking the activation of IKKβ. A number of compounds with plausible therapeutic potential in inflammatory and proliferative disorders, including aspirin, sodium salicylate, sulindac, arsenic trioxide, SPC 839, PS-1145, ML120B, SC-514, BMS-345541, CHS 828 and IMD-0354, have been shown to inhibit IKKβ (Schmid and Birbach, 2008). Also, some extracts including *Euonymus alatus* (Oh et al., 2010), and pure compounds including tanshinone IIA (Jang et al., 2006), artemisolide (Kim et al., 2007), asiatic acid (Yun et al., 2008), and miyabenol A (Ku et al., 2008) from natural sources showed IKK inhibition.

Therefore, this is an interesting mechanistic relationship that suggests epimuqubilin A warrants further exploration as a potential anti-inflammatory or cancer chemopreventive agent.

4. Experimental

4.1. Reagents

Epimuqubilin A (Fig. 1A) was isolated as previously described (Cheenpracha et al., 2010). Lipopolysaccharide (LPS), and sulforhodamine B (SRB) were purchased from Sigma–Aldrich Co. (St. Louis, MO, USA). Cell lysis buffer (10×), rabbit monoclonal antibodies against GAPDH, phospho (p)-p44/42 MAPK (ERK1/2) (Thr202/Tyr204), ERK1/2, p-p38 MAPK (Thr180/Tyr182), p-SAPK/JNK (Thr183/Tyr185), SAPK/JNK, and p-IκB kinase (IKK) (Ser176/180), rabbit polyclonal antibodies against β-actin, COX-2, IκB-α, p38 MAPK, and NF-κB p65, and anti-rabbit IgG, HRP-linked antibody were purchased from Cell Signaling Technology (Beverly, MA, USA). Rabbit polyclonal antibody against lamin A/C was purchased from Santa Cruz Biotechnology (Santa Cruz, CA). Rabbit polyclonal anti-iNOS antibody was purchased from Abcam Inc. (Cambridge, MA, USA). Enhanced chemiluminescence (ECL) detection kit was purchased from Amersham Biosciences (Piscataway, NJ, USA). Dulbecco's Modified Eagle's Medium (DMEM), fetal bovine serum (FBS), antibiotics–antimycotics (100 U/ml penicillin G sodium, 100 μg/ml streptomycin sulfate and 0.25 μg/ml amphotericin B), oligonucleotide PCR primers, and Trizol® reagent were purchased from Invitrogen™ (Carlsbad, CA, USA). RT^2 First Strand Kit (C-03) was purchased from SABiosciences™ (Frederick, MD, USA). PerfeCTa™ SyBR® Green FastMix™, ROX was purchased from Quanta Biosciences™ (Gaithersburg, MD, USA). IRDye® 700 infrared dye-5′-end-labelled NF-κB oligonucleotide was purchased from Integrated DNA Technologies Inc. (Coralville, IA, USA).

4.2. Cell culture

RAW 264.7 murine macrophage cells were cultured in DMEM supplemented with 10% heat-inactivated FBS and antibiotics–antimycotics at 37 °C in a 5% CO_2 humidified incubator.

4.3. Measurement of nitrite production

The level of nitrite, the stable end product of NO, was measured as described previously (Cheenpracha et al., 2010). In brief, RAW 264.7 cells (1×10^4 cells/well) were seeded and incubated in 96-well culture plates at 37 °C, 5% CO_2 in a humidified air for 24 h. Then, complete medium was replaced with phenol red-free medium containing various concentrations of epimuqubilin A, followed by treatment with 1 μg/ml of LPS for 20 h. The nitrite released in the culture media was reacted with Griess reagent and the absorbance was

measured at 540 nm. The amount of nitrite was calculated using a standard curve of the known nitrite concentration versus absorbance at 540 nm. Under the same experimental conditions, SRB assays were performed to evaluate the cytotoxic effect of epimuqubilin A toward RAW 264.7 cells (You et al., 1995.).

4.4. Western blot analyses

Cells were harvested and lysed using 1× cell lysis buffer according to the manufacturer's instructions. After 5 min of incubation with lysis buffer, cells were centrifuged at 14,000 × *g* for 10 min at 4 °C, and the supernatant as cell lysate was collected and stored at −80 °C until use. After quantification of protein using Bradford reagent (Bradford, 1976), equal amounts of total protein in each cell lysate were resolved using SDS-PAGE, and electro-transferred to PVDF membranes. The membranes were incubated with 5% skimmed milk in 0.1% Tween 20 containing TBS for 1 h at room temperature to block non-specific protein binding. Then, membranes were incubated overnight at 4 °C with corresponding primary antibodies in 3% skimmed milk in TBS followed by incubation with horseradish peroxidase-conjugated secondary antibodies, and visualization using an ECL detection kit according to the manufacturer's instructions with a Geliance 1000 imager (Perkin Elmer, Inc., Waltham, MA, USA). Band densities were quantified using ImageJ software from the National Institutes of Health and quantified as a fold-change compared with control after the normalization to an internal standard μ-actin.

4.5. Quantitative real time-polymerase chain reaction (RT-PCR) analysis

As described previously, total RNA was extracted from cells using Trizol® reagent according to the manufacturer's instructions based on the method of Chomczynski and Sacchi (1987). Isolated RNA was dissolved in RNase-free water and the absorbance was measured at 230, 260, and 280 nm to determine the quality (A260/230, A260/280) and quantity (A260) of purified RNA, using a NanoDrop ND-1000 spectrophotometer (Thermo Fisher Scientific Inc., Wilmington, DE, USA). After incubation with genomic DNA elimination mixture at 42 °C for 5 min, total RNA (1 μg) was mixed with reagents of RT^2 First Strand Kit (C-03) according to the manufacturer's instructions and cDNA was generated by reverse transcription under the condition of 42 °C for 15 min and 95 °C for 5 min using RT^2 First Strand Kit (C-03) with an ABI 7300 thermocycler (Applied Biosystems Inc., Foster City, CA, USA). cDNA was amplified using 2× PerfeCTa™ SyBR® Green FastMix™, ROX reagent, with corresponding primer pairs as follows: iNOS: 5′-GGAGCGAGTTGTGGATTGTC-3′ (sense) and 5′-GTGAGGGCTTGGCTGAGTGAG-3′ (antisense); COX-2: 5′-GAAGTCTTTGGTCTGGTGCCTG-3′ (sense) and 5′-GTCTGCTGGTTTGGAATAGTTGC-3′ (antisense); βactin: 5′-GCTACAGCTTCACCACCACAG-3′ and 5′-GGTCTTTACGGATGTCAACGTC-3′ (antisense) (Zhao et al., 2010). The PCR was conducted under the following conditions: initial denaturation step at 94 °C for 3 min, repeated cycling (50 times) step of denaturation at 94 °C for 30 s, annealing at 57 °C for 30 s, and elongation at 72 °C for 30 s. mRNA expression level of COX-2 or iNOS was normalized to that of β-actin. The signal was collected at the end of each cycle and fold changes were calculated based on the $2^{-\Delta\Delta CT}$ method (Zhao et al., 2010).

4.6. Preparation of nuclear extracts and electrophoretic mobility shift assay (EMSA)

Nuclear extracts were prepared as previously described (Park et al., 2005). Briefly, PBS-washed cells were incubated in EMSA lysis buffer (10 mM Tris–HCl, pH 8.0, 60 mM KCl, 1 mM EDTA, 1 mM dithiothreitol, 100 mM PMSF, and 0.1% NP-40) for 5 min on ice. Following centrifugation at 2500 rpm at 4 °C for 4 min, the pellet was washed with lysis buffer without NP-40. The nuclear proteins were extracted from the pellet after 10 min incubation with nuclear extract buffer (20 mM Tris–HCl, pH 8.0, 420 mM NaCl, 1.5 mM

$MgCl_2$, 0.2 mM EDTA and 25% glycerol) and centrifugation at 14,000 rpm at 4 °C for 15 min. Binding reactions were performed by incubation of 5 μg of nuclear protein extracts, 2.5 mM dithiothreitol, 1 μg of poly (dI–dC), 2.5% glycerol, 50 mM KCl, 10 mM EDTA, and 50 nM IRDye® 700 infrared dye-5′-end-labelled NF-κB oligonucleotides for 30 min at room temperature. Protein–DNA complexes were resolved by electrophoresis on 5% polyacrylamide gels in 1× TGE buffer at 70 V for 1 h. The gel was visualized using an Odyssey® Infrared Imaging System (LI-COR Biosciences, Lincoln, NE, USA).

4.7. Statistical analysis

Data were expressed as means ± standard deviation (SD). One-way ANOVA followed by Tukey's *post hoc* test was used for the determination of statistical comparisons (SigmaPlot 12, Systat Software Inc.). *P* values less than 0.05 were considered statistically significant.

Acknowledgments

The work was supported in part by program project P01 CA48112 awarded by the National Cancer Institute and support provided by the Cancer Research Center Hawaii.

References

1. Aggarwal BB, Gehlot P. Inflammation and cancer: how friendly is the relationship for cancer patients? Curr. Opin. Pharmacol. 2009; 9:351–369. [PubMed: 19665429]
2. Ambs S, Merriam WG, Bennett WP, Felley-Bosco E, Ogunfusika MO, Oser SM, Klein S, Shields PG, Billiar TR, Harris CC. Frequent nitric oxide synthase-2 expression in human colon adenomas: implication for tumor angiogenesis and colon cancer progression. Cancer Res. 1998; 58:334–341. [PubMed: 9443414]
3. Azevedo LG, Peraza GG, Lerner C, Soares A, Murcia N, Muccillo-Baisch AL. Investigation of the anti-inflammatory and analgesic effects from an extract of *Aplysina caissara*, a marine sponge. Fundam. Clin. Pharmacol. 2008; 22:549–556. [PubMed: 18844726]
4. Bradford MM. A rapid and sensitive method for the quantitation of microgram quantities of protein utilizing the principle of protein-dye binding. Anal. Biochem. 1976; 72:248–254. [PubMed: 942051]
5. Broholm H, Rubin I, Kruse A, Braendstrup O, Schmidt K, Skriver EB, Lauritzen M. Nitric oxide synthase expression and enzymatic activity in human brain tumors. Clin. Neuropathol. 2003; 22:273–281. [PubMed: 14672505]
6. Cheenpracha S, Park EJ, Rostama B, Pezzuto JM, Chang LC. Inhibition of nitric oxide (NO) production in lipopolysaccharide (LPS)-activated murine macrophage RAW 264.7 cells by the norsesterterpene peroxide, epimuqubilin A. Mar. Drugs. 2010; 8:429–437. [PubMed: 20411107]
7. Chomczynski P, Sacchi N. Single-step method of RNA isolation by acid guanidinium thiocyanate–phenol–chloroform extraction. Anal. Biochem. 1987; 162:156–159. [PubMed: 2440339]
8. Dai J, Liu Y, Zhou YD, Nagle DG. Hypoxia-selective antitumor agents: norsesterterpene peroxides from the marine sponge *Diacarnus levii* preferentially suppress the growth of tumor cells under hypoxic conditions. J. Nat. Prod. 2007; 70:130–133. [PubMed: 17253866]
9. Ekmekcioglu S, Ellerhorst JA, Prieto VG, Johnson MM, Broemeling LD, Grimm EA. Tumor iNOS predicts poor survival for stage III melanoma patients. Int. J. Cancer. 2006; 119:861–866. [PubMed: 16557582]
10. El Sayed KA, Hamann MT, Hashish NE, Shier WT, Kelly M, Khan AA. Antimalarial, antiviral, and antitoxoplasmosis norsesterterpene peroxide acids from the Red Sea sponge *Diacarnus erythraeanus*. J. Nat. Prod. 2001; 64:522–524. [PubMed: 11325240]
11. Ferreiro DU, Komives EA. Molecular mechanisms of system control of NF-κB signaling by IκBα. Biochemistry. 2010; 49:1560–1567. [PubMed: 20055496]
12. Förstermann U. Nitric oxide and oxidative stress in vascular disease. Pflugers Arch. 2010; 459:923–939. [PubMed: 20306272]

13. Fukumura D, Kashiwagi S, Jain RK. The role of nitric oxide in tumour progression. Nat. Rev. Cancer. 2006; 6:521–534. [PubMed: 16794635]
14. Greenhough A, Smartt HJ, Moore AE, Roberts HR, Williams AC, Paraskeva C, Kaidi A. The COX-2/PGE_2 pathway: key roles in the hallmarks of cancer and adaptation to the tumour microenvironment. Carcinogenesis. 2009; 30:377–386. [PubMed: 19136477]
15. Hayashi H, Kuwahara M, Fujisaki N, Furihata M, Ohtsuki Y, Kagawa S. Immunohistochemical findings of nitric oxide synthase expression in urothelial transitional cell carcinoma including dysplasia. Oncol. Rep. 2001; 8:1275–1279. [PubMed: 11605048]
16. Hussain SP, Harris CC. Inflammation and cancer: an ancient link with novel potentials. Int. J. Cancer. 2007; 121:2373–2380. [PubMed: 17893866]
17. Ibrahim SR, Ebel R, Wray V, Müller WE, Edrada-Ebel R, Proksch P. Diacarperoxides, norterpene cyclic peroxides from the sponge *Diacarnus mega-spinorhabdosa*. J. Nat. Prod. 2008; 71:1358–1364. [PubMed: 18672931]
18. Jang SI, Kim HJ, Kim YJ, Jeong SI, You YO. Tanshinone IIA inhibits LPS-induced NF-kappaB activation in RAW 264.7 cells: possible involvement of the NIK-IKK, ERK1/2, p38 and JNK pathways. Eur. J. Pharmacol. 2006; 542:1–7. [PubMed: 16797002]
19. Kanwar JR, Kanwar RK, Burrow H, Baratchi S. Recent advances on the roles of NO in cancer and chronic inflammatory disorders. Cur. Med. Chem. 2009; 16:2373–2394.
20. Kim BH, Lee JY, Seo JH, Lee HY, Ryu SY, Ahn BW, Lee CK, Hwang BY, Han SB, Kim Y. Artemisolide is a typical inhibitor of IκB kinase beta targeting cysteine-179 residue and down-regulates NF-κB-dependent TNF-alpha expression in LPS-activated macrophages. Biochem. Biophys. Res. Commun. 2007; 361:593–598. [PubMed: 17669364]
21. Ku KT, Huang YL, Huang YJ, Chiou WF. Miyabenol A inhibits LPS-induced NO production via IKK/IκB inactivation in RAW 264.7 macrophages: possible involvement of the p38 and PI3K pathways. J. Agric. Food Chem. 2008; 56:8911–8918. [PubMed: 18783239]
22. Li Q, Verma IM. NF-κB regulation in the immune system. Nat. Rev. Immunol. 2002; 2:725–734. [PubMed: 12360211]
23. Liu SF, Malik AB. NF-κB activation as a pathological mechanism of septic shock and inflammation. Am. J. Physiol. Lung Cell. Mol. Physiol. 2006; 290:L622–L645. [PubMed: 16531564]
24. Mayer AM, Glaser KB, Cuevas C, Jacobs RS, Kem W, Little RD, McIntosh JM, Newman DJ, Potts BC, Shuster DE. The odyssey of marine pharmaceuticals: a current pipeline perspective. Trends Pharmacol. Sci. 2010; 31:255–265. [PubMed: 20363514]
25. Oeckinghaus A, Ghosh S. The NF-κB family of transcription factors and its regulation. Cold Spring Harb. Perspect. Biol. 2009; 1:a000034. [PubMed: 20066092]
26. Oh BK, Mun J, Seo HW, Ryu SY, Kim YS, Lee BH, Oh KS. Euonymus alatus extract attenuates LPS-induced NF-κB activation via IKKβ inhibition in RAW 264.7 cells. J. Ethnopharmacol. 2010
27. Park HJ, Chung HJ, Min HY, Park EJ, Hong JY, Kim WB, Kim SH, Lee SK. Inhibitory effect of DA-125, a new anthracyclin analog antitumor agent, on the invasion of human fibrosarcoma cells by down-regulating the matrix metalloproteinases. Biochem. Pharmacol. 2005; 71:21–31. [PubMed: 16271263]
28. Pautz A, Art J, Hahn S, Nowag S, Voss C, Kleinert H. Regulation of the expression of inducible nitric oxide synthase. Nitric Oxide. 2010; 23:75–93. [PubMed: 20438856]
29. Phuwapraisirisan P, Matsunaga S, Fusetani N, Chaitanawisuti N, Kritsanapuntu S, Menasveta P. Mycaperoxide, Ha new cytotoxic norsesterterpene peroxide from a Thai marine sponge Mycale sp. J. Nat. Prod. 2003; 66:289–291. [PubMed: 12608869]
30. Rajnakova A, Moochhala S, Goh PM, Ngoi S. Expression of nitric oxide synthase, cyclooxygenase, and p53 in different stages of human gastric cancer. Cancer Lett. 2001; 172:177–185. [PubMed: 11566494]
31. Schmid JA, Birbach A. IκB kinase β (IKK β/IKK2/IKBKB) – a key molecule in signaling to the transcription factor NF-κB. Cytokine Growth Factor Rev. 2008; 19:157–165. [PubMed: 18308615]
32. Schumacher M, Cerella C, Eifes S, Chateauvieux S, Morceau F, Jaspars M, Dicato M, Diederich M. Heteronemin, a spongean sesterterpene, inhibits TNFα-induced NF-κB activation through

proteasome inhibition and induces apoptotic cell death. Biochem. Pharmacol. 2010; 79:610–622. [PubMed: 19814997]

33. Sperry S, Valeriote FA, Corbett TH, Crews P. Isolation and cytotoxic evaluation of marine sponge-derived norterpene peroxides. J. Nat. Prod. 1998; 61:241–247. [PubMed: 9514009]
34. Thomas TR, Kavlekar DP, LokaBharathi PA. Marine drugs from sponge-microbe association – a review. Mar. Drugs. 2010; 8:1417–1468. [PubMed: 20479984]
35. Tsubosaka Y, Murata T, Yamada K, Uemura D, Hori M, Ozaki H. Halichlorine reduces monocyte adhesion to endothelium through the suppression of nuclear factor-κB activation. J. Pharmacol. Sci. 2010; 113:208–213. [PubMed: 20562517]
36. Wilson KT, Fu S, Ramanujam KS, Meltzer SJ. Increased expression of inducible nitric oxide synthase and cyclooxygenase-2 in Barrett's esophagus and associated adenocarcinomas. Cancer Res. 1998; 58:2929–2934. [PubMed: 9679948]
37. Yang JH, Suh SJ, Lu Y, Li X, Lee YK, Chang YC, Na MK, Choi JH, Kim CH, Son JK, Chang HW. Anti-inflammatory activity of ethylacetate fraction of *Cliona celata*. Immunopharmacol. Immunotoxicol. 2010 (Epub ahead of print).
38. Yasuhara-Bell J, Lu Y. Marine compounds and their antiviral activities. Antiviral Res. 2010; 86:231–240. [PubMed: 20338196]
39. You M, Wickramaratne DB, Silva GL, Chai H, Chagwedera TE, Farnsworth NR, Cordell GA, Kinghorn AD, Pezzuto JM. (−)-Roemerine, an aporphine alkaloid from *Annona senegalensis* that reverses the multidrug-resistance phenotype with cultured cells. J. Nat. Prod. 1995; 58:598–604. [PubMed: 7623038]
40. Youssef DT. Tasnemoxides A–C, new cytotoxic cyclic norsesterterpene peroxides from the Red Sea sponge *Diacarnus erythraenus*. J. Nat. Prod. 2004; 67:112–114. [PubMed: 14738401]
41. Youssef DT, Yoshida WY, Kelly M, Scheuer PJ. Cytotoxic cyclic norterpene peroxides from a Red Sea sponge *Diacarnus erythraenus*. J. Nat. Prod. 2001; 64:1332–1335. [PubMed: 11678661]
42. Yun KJ, Kim JY, Kim JB, Lee KW, Jeong SY, Park HJ, Jung HJ, Cho YW, Yun K, Lee KT. Inhibition of LPS-induced NO and PGE_2 production by asiatic acid via NF-κB inactivation in RAW 264.7 macrophages: possible involvement of the IKK and MAPK pathways. Int. Immunopharmacol. 2008; 8:431–441. [PubMed: 18279797]
43. Zhao L, Tao JY, Zhang SL, Jin F, Pang R, Dong JH. n-Butanol extract from *Melilotus suaveolens* Ledeb affects pro- and anti-inflammatory cytokines and mediators. Evid. Based Complement. Alternat. Med. 2010; 7:97–106. [PubMed: 18955281]

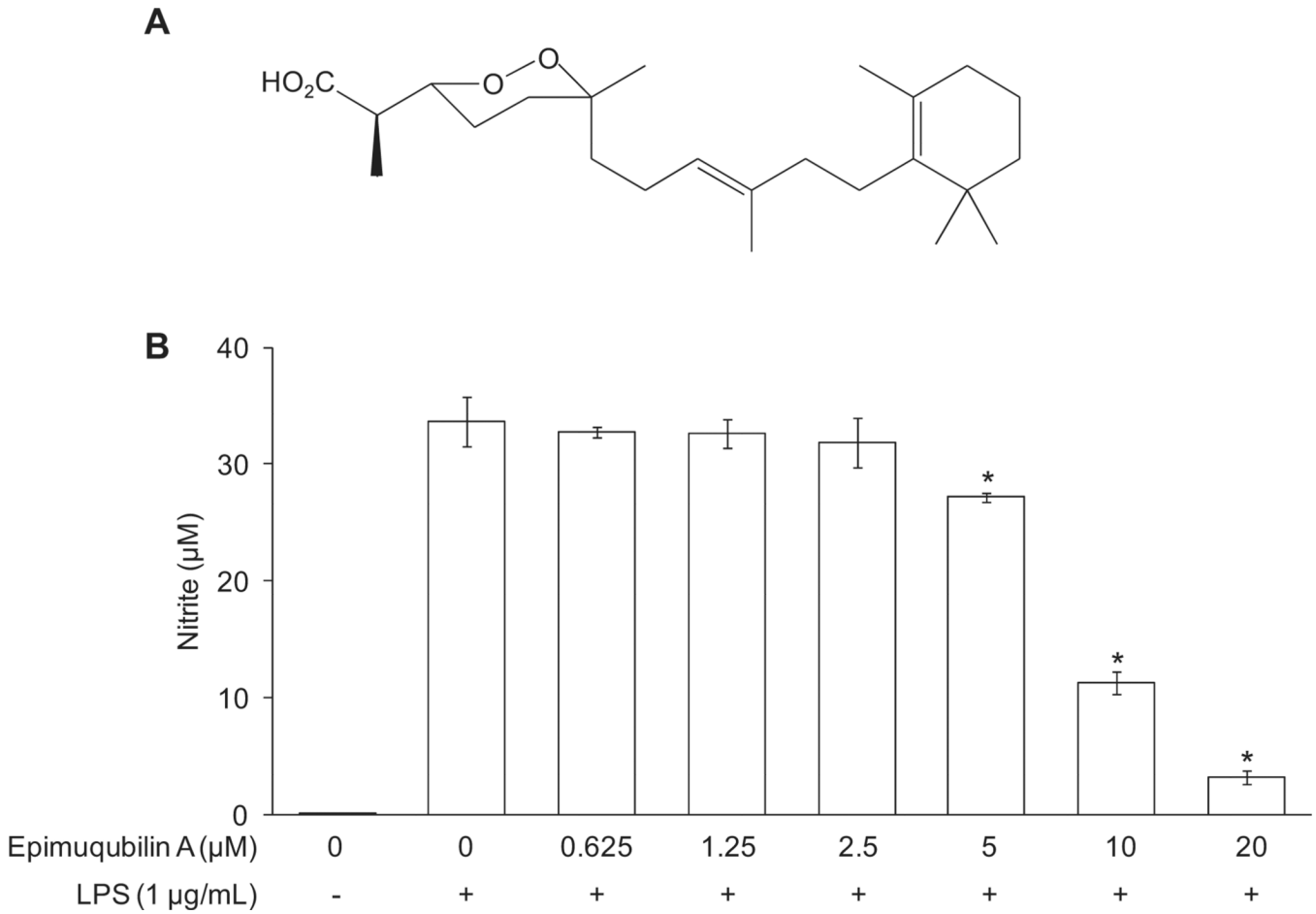

Fig. 1.

Concentration-dependent inhibitory effects of epimuqubilin A on LPS-induced NO production in RAW 264.7 cells. (A) Chemical structure of epimuqubilin A. (B) Cells were pretreated with the indicated concentrations (0–20 μM) of epimuqubilin A for 15 min, and then stimulated with LPS for 20 h. The level of nitrite produced by LPS treatment was significantly suppressed by each concentration of epimuqubilin A. An asterisk (*) indicates a significant difference between the respective groups with *P* values less than 0.05.

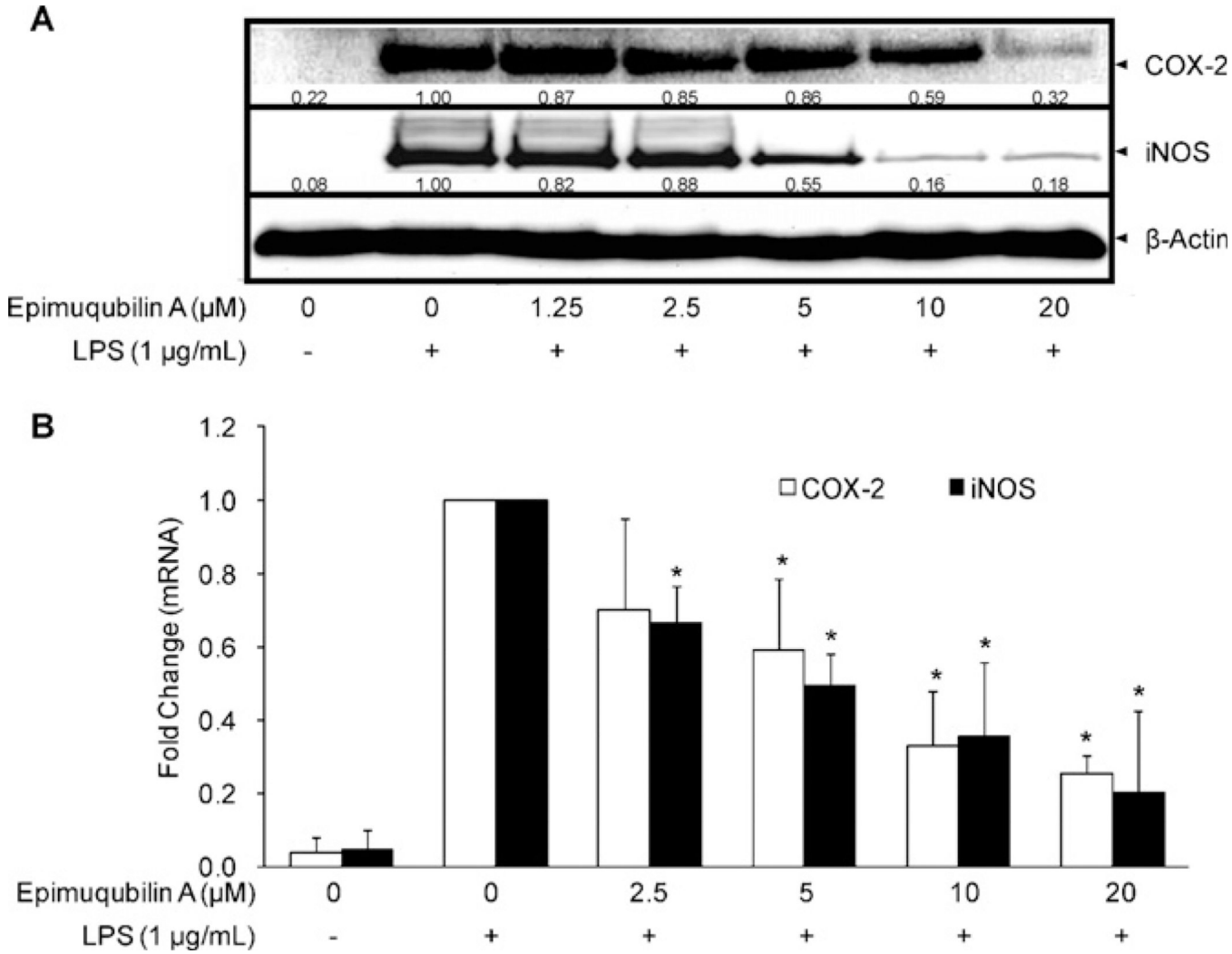

Fig. 2.

Effect of epimuqubilin A on iNOS and COX-2 protein expression and RNA levels. (A) Inhibitory effect of epimuqubilin A on COX-2 and iNOS protein expression. RAW 264.7 cells were pretreated with the indicated concentrations of epimuqubilin A (0–20 μM) for 15 min, and then stimulated with LPS (1 μg/mL). After an 18 h incubation period, cells were lysed, and 15 μg protein was applied on a 9% SDS-polyacrylamide gel. The levels of COX-2 and iNOS protein expression were examined by Western blot analyses using antibodies against COX-2 or iNOS. β-Actin was used as an internal standard. (B) Inhibitory effect of epimuqubilin A on COX-2 (open bars) and iNOS (closed bars) mRNA levels. RAW 264.7 cells were pretreated with the indicated concentrations of epimuqubilin A (0–20 μM) for 15 min, and then stimulated with 1 μg/ml LPS. After a 5 h incubation period, RNA was extracted and quantified. Total RNA (1 μg) was used in the RT-PCR; primers are specified in Section 4.5. After normalization to the internal standard, β-actin, fold-changes relative to vehicle-treated control is presented ($n = 3$). An asterisk (*) indicates a significant difference with P values less than 0.05.

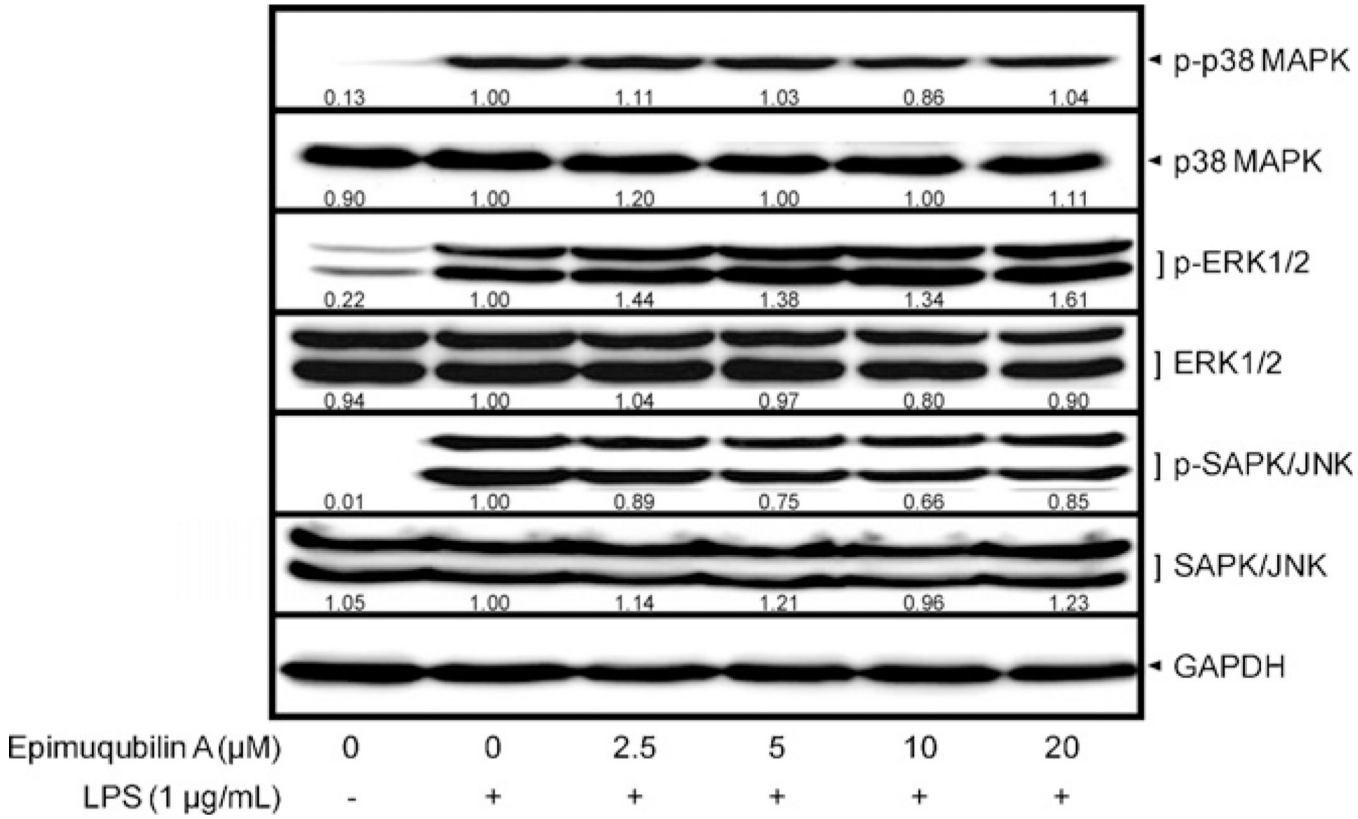

Fig. 3.

Effect of epimuqubilin A on LPS-induced MAPKs activation in cultured RAW 264.7 cells. RAW 264.7 cells were pretreated with various concentrations up to 20 μM of epimuqubilin A for 15 min, and then incubated with LPS (1 μg/mL) for 15 min. Total cell lysate was prepared and the levels of p-p38 MAPK, total p38 MAPK, p-ERK1/2, total ERK1/2, p-SAPK/JNK, and SAPK/JNK were analyzed by Western blotting. The band intensities were normalized to that of the β-actin; data are presented as fold-changes.

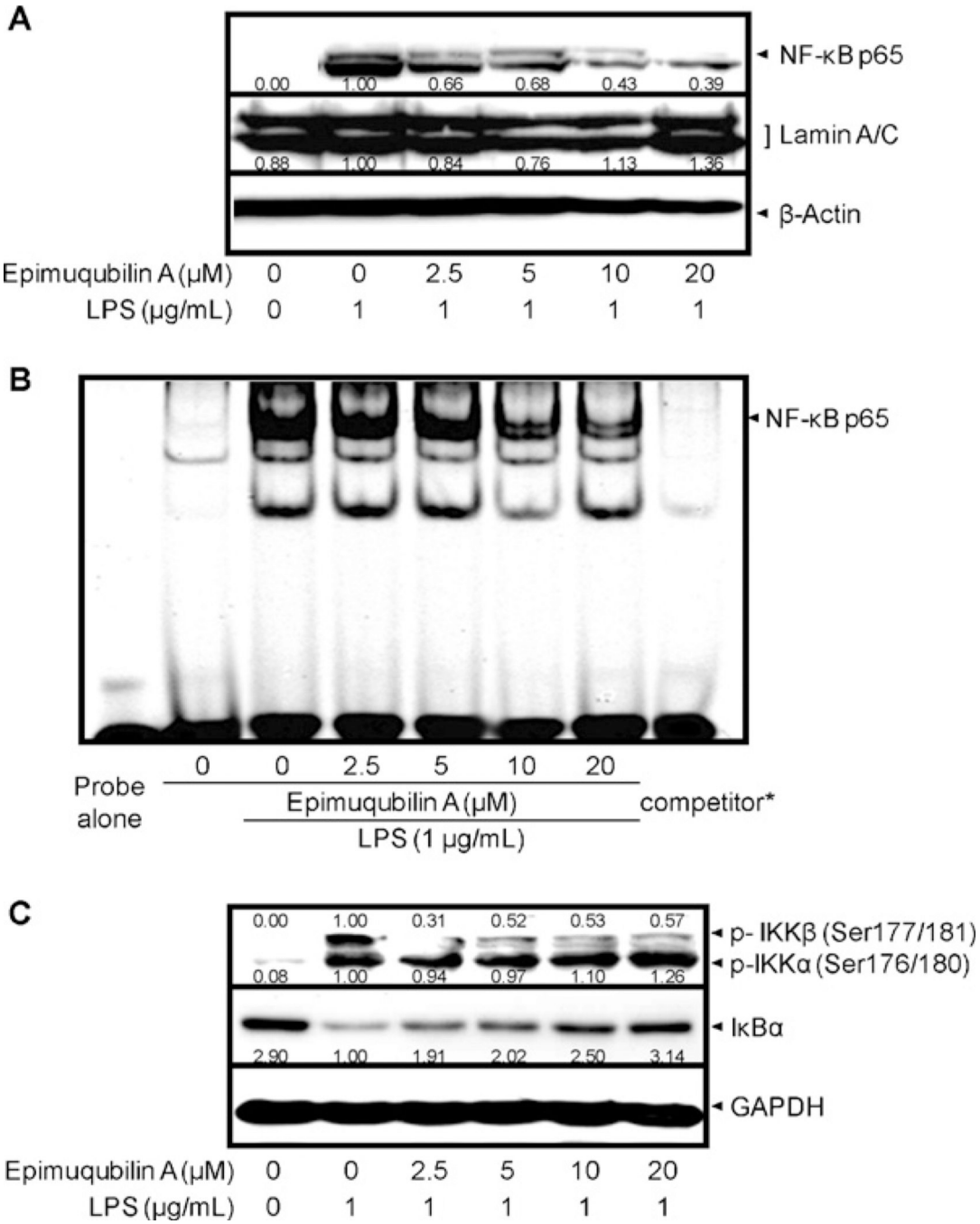

Fig. 4.

Effect of epimuqubilin A on LPS-induced IκBα degradation, NF-κB nuclear translocation, NF-κB DNA binding, and IKKα/β phosphorylation in cultured RAW 264.7 cells. (A) Cells were pretreated with the indicated concentrations of epimuqubilin A for 15 min, incubated with LPS for 1 h, and nuclear fractions were extracted and the protein level of NF-κB p65 was analyzed by Western blotting. Band intensities were normalized to that of the β-actin; data are presented as fold-changes. (B) RAW 264.7 cells were pretreated with the indicated concentrations of epimuqubilin A for 15 min, and then stimulated with LPS (1 μg/mL) for 1.5 h. Nuclear fractions were prepared as described in Section 4. The NF-κB protein–DNA binding complex was resolved in 5% polyacrylamide gel and visualized with an Odyssey®

Infrared Imaging System. *During the binding reaction, a concentrated NF-κB specific unlabeled consensus (10 μM, 200×) was added to verify the specific NF-κB protein–DNA interaction. (C) After pretreatment with the indicated concentration of epimuqubilin A for 15 min followed by incubation with LPS (1 μg/mL) for 15 min, cells were lysed and protein levels of p-IKKα/β and IκBα were analyzed by Western blotting. Band intensities were normalized to that of the β-actin; data are presented as fold-changes.